J Appl Electrochem (2008) 38:759–766
DOI 10.1007/s10800-008-9505-7

ORIGINAL PAPER

Thin-film composite nanofiltration membranes prepared by electropolymerization

Robert Gloukhovski · Yoram Oren · Charles Linder · Viatcheslav Freger

Received: 6 August 2007 / Revised: 25 January 2008 / Accepted: 28 January 2008 / Published online: 13 February 2008

Abstract A novel approach to preparation of composite asymmetric nanofiltration membranes is reported based on a thin selective layer deposited by electropolymerization (EP) on top of an asymmetrically porous and electronically conductive porous support. Support films with ultrafiltration characteristics were cast from a concentrated dispersion of carbon black particles, a few tens of nanometers large, in a solution of polysulfone followed by precipitation in a non-solvent bath (phase inversion). Composite membranes with poly(phenylene oxide) and polyaniline thin top layers were prepared by EP deposition from solutions of phenol and aniline, respectively, of which polyaniline film demonstrated a dense uniform structure and water flux and rejection to sucrose and magnesium sulfate in the nanofiltration range.

Keywords Electropolymerization · Nanofiltration · Water treatment · Polyaniline · Polyethylene oxide · Thin-film composite membranes

R. Gloukhovski · C. Linder · V. Freger (✉)
The Department of Biotechnology Engineering, Ben Gurion University of The Negev, P.O. Box 653, Beer Sheva 84105, Israel
e-mail: vfreger@bgu.ac.il

Y. Oren · C. Linder · V. Freger
The Zuckerberg Institute for Water Research, Ben Gurion University of The Negev, P.O. Box 653, Beer Sheva 84105, Israel

Y. Oren
Unit of Environmental Engineering, Ben Gurion University of The Negev, P.O. Box 653, Beer Sheva 84105, Israel

1 Introduction

Nanofiltration (NF) and reverse osmosis (RO) separate or remove small molecules and ions (<1000 Da) from a solvent (most often water) by means of pressure-driven filtration through a dense polymeric membrane. They have a wide range of applications in desalination and treatment of aqueous streams in the pulp and paper, textile and food industries, biotechnology etc. [1–3]. Combination of selectivity with high permeability to water and mechanical strength sufficient to withstand high pressures is achieved by using thin-film composite (TFC) membranes comprising a dense film of 10–200 nm (active layer) supported by a thick asymmetric porous film. This asymmetric film is characterized by morphology where its pore size gradually decreases towards the active layer from a few tens of microns down to about a nanometer. For the overall performance of the composite it is critical that the active layer possess good uniformity with minimal thickness and a negligible fraction of defects over its entire surface, which is commonly many square meters per unit. The superior method of producing defect-free thin films is interfacial polymerization (IP), whereby a thin polyamide film is formed between two immiscible solutions containing multifunctional condensation monomers reacting at interface [4, 5]. IP is inherently self-limiting thus yielding very thin films and self-healing, which results in low defect rate. It offers an additional option to control polymer morphology (amorphous vs. crystalline), cross-linking density and, ultimately, membrane permeability by varying average monomer functionality.

However, the use of IP is restricted to a few classes of condensation polymers, of which only some polyamides have in fact been used. Despite excellent performance, polyamides have some disadvantages, such as the low

tolerance to oxidants, in particular chlorine [4, 5], which precludes the use of chlorine for disinfection and makes the membranes prone to biofouling, which reduces performance and shortens lifetime [3, 6, 7]. In addition, polyamides prove to be insufficiently selective for some solutes (borates, urea, hormones, and many other small organics) [3, 8, 9]. This motivates the search for alternative materials and approaches for large-scale production of supported defect-free films with a thickness in the meso- or nano-scopic range that would match the excellence of IP.

This work explores a novel approach to fabrication of such selective films. The central idea is to replace IP with electrochemical polymerization (EP) on an electronically conductive substrate [10]. Compared to IP, EP employs different types of monomers and polymers, which makes it attractive for producing new types of desalination and separation membranes with different stabilities and selectivities. Another advantage, unavailable in IP, is that applied electric potential may be a convenient means to control membrane chemistry and cross-linking.

However, to be a suitable support for the EP film formed from either monomer requires that the substrate be electronically conductive in addition to its normal characteristic of being asymmetrically porous. It is crucial that the conductivity and porosity at the top surface be uniform down to the nanometer scale to ensure formation of a uniform film of nanoscale thickness. For this reason, two distinct steps had to be considered in this study, namely

(a) preparation of a film, both conductive and asymmetrically porous, that would serve as substrate for EP-deposition and, subsequently, as a support for the top layer;
(b) EP deposition of a selective top layer of a nanoscale thickness and possessing characteristic of nanofiltration or reverse osmosis.

Due to the exploratory nature of this work, it was limited to only a few materials pertaining to each step. In choosing the materials and procedures, we attempted, on one hand, to take maximal advantage of the existing technological solutions for preparing efficient supporting films and, on the other hand, to cover the most typical situations and analyze possible limitations faced while carrying out this general approach.

2 Experimental

2.1 Materials

Conductive fillers—carbon blacks Vulcan P (Cabot, surface area 700 $m^2\ g^{-1}$), Black Pearl 2000 (Cabot, surface area 1700 $m^2\ g^{-1}$), carbon nanofibers of diameter 80–150 nm, >10 μm long (graphitized nanofibers, grade ENF-100AA-GFE, Electrovac, Austria) and matrix polymer—PSf (UDEL 3500, Solvay Advanced Polymers) were dried in an oven at 150 °C overnight prior to use. N-methyl-2-pyrrolidone (NMP, Merck), non-woven polyester fabric (Awa Paper, Japan), dispersing agents—poly(vinyl pyrrolidone) (PVP, 40 kDa), polyethylene-*block*-poly(ethylene oxide) (PE-*b*-PEO, ~575 Da, 20% ethylene oxide) and polystyrene-*block*-polybutadiene (PS-*b*-PB, ca. 20% styrene), Dextran (40 kDa) and other materials (all purchased from Aldrich) were used as received.

2.2 Preparation of the conductive support

The following procedure was found to yield supports with a reasonable combination of properties. The conductive filler was dispersed in NMP at 100 °C by mechanical stirring using a blade stirrer for about 4 h (if a dispersion agent was used, it was dissolved in NMP prior to conductive filler addition). This was followed by addition and dissolution of PSf for another 4 h until a homogeneous mixture was obtained. (Note that reverse order, i.e., addition of CB to a PSf solution, failed to produce a good dispersion.) Using a stainless steel casting bar, the mixture was used to cast a 400 μm thick film onto a non-woven fabric attached to a glass plate. In order to achieve a narrower pore-size in the top layer, an intermediate solvent evaporation step was carried out in an oven at 110 °C for 5 min, followed by polymer precipitation by immersing the glass plate into ice-cold water bath overnight for complete leaching of the solvent. Dense composite films were prepared as well following essentially the same procedure without immersion precipitation step and the solvent was simply evaporated in oven at 110 °C overnight. The obtained supports that were detached from the glass plates were stored in 1% sodium metabisulfite solution to prevent bacteria growth.

2.3 Film deposition

Deposition of an active layer by means of EP on the top surface of a support prepared as described above was carried out in a setup shown in Fig. 1. A circular piece of diameter ca. 55 mm was cut from the conductive support and placed at the bottom of the electrochemical cell (a hollow cylinder made of Perspex). The inner part of diameter 41 mm (13.2 cm^2) was sealed with an O-ring and served as anode, while current was collected through the dry outer edge clamped with a concentric stainless steel ring connected to a PCI4 potentiostat (Gamry Instruments-USA). A circular piece of platinum mesh of a diameter

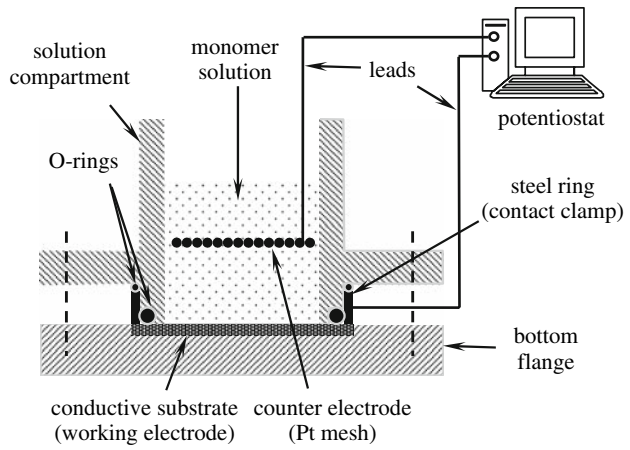

Fig. 1 Schematic drawing of the setup for toplayer deposition by means of electropolymerization on top of conductive porous substrate (support)

slightly smaller than the inner diameter of the cell was placed horizontally inside the cell ca. 10 mm above the bottom and served both as a counter electrode and a pseudoreference. The cell was filled with about 25 mL of solution containing a monomer and the supporting electrolyte, which covered both electrodes and the relevant electrochemical procedure, was applied. The obtained composite membranes were washed thoroughly with deionized water prior to further examination and high resolution SEM (HR-SEM) observations.

2.4 Determination of transport properties

The filtration tests were carried out in a magnetically stirred filtration cell (9.6 cm^2 area) made of stainless steel and pressurized with nitrogen from a gas cylinder. The pressure was 5 bar for support films and 10 bar for composite membranes. Hydraulic permeability (flux) was evaluated by filtration of deionized water. Rejection tests employed 3% dextran solution, 0.5% sucrose solution and 0.01 M $MgSO_4$ solution. Dextran concentration was analyzed an OPTECH portable refractometer, sucrose—by a TOC-5000A analyzer (Shimadzu) and magnesium sulfate—by an InoLab Cond Level 1 conductivity meter.

3 Results and discussion

3.1 General considerations and the choice of materials

We chose to prepare the substrate by using carbon particles a few tens of nanometers large as conductive filler for the polysulfone (PSf), a standard polymer for casting asymmetric porous supports for thin-film composite (TFC) membranes. Conductive composite materials comprising polymers and carbon black particles [11] have been actively investigated for various applications [12, 13]. They can be prepared by various methods and demonstrate electronic conductivity up to 1 S cm^{-1} [14–16]. The present work required the highest possible conductivity in order to keep the whole surface at a nearly uniform potential and ensure uniform top layer deposition by EP. A circular piece of substrate of diameter D electrically connected (clamped) at the edges and collecting a uniform current density i all over its surface will require a specific conductivity (see Appendix for derivation)

$$\sigma_{\min} = iD^2/16h\Delta\varphi, \quad (1)$$

where h is the substrate thickness and $\Delta\varphi$ is the maximum allowed potential variation along the substrate. Other geometries simply change the factor, e.g., to 1/8 for a rectangular clamped at opposite edges. Typical values used here $i = 3$ mA cm^{-2}, $h = 200$ μm, $D = 40$ mm, and $\Delta\varphi < 0.5$ V then require $\sigma > 0.3$ S cm^{-1}, which is an achievable value: this suggests that the highest possible carbon content has to be used. Obviously a setup in which current is collected across rather than along the substrate may drastically reduce the required $\sigma_{\min}$. Yet, since the porous film is normally cast onto an insulating polymeric non-woven fabric, clamping at the edges seems to be technologically more appealing and therefore we focused on this more demanding (in terms of conductivity) configuration.

The electrical conductivity of polymer-carbon composites depends critically on the volume fraction of the conductive fillers particles and is well explained by the percolation theory [17]. Above a critical concentration (a percolation threshold) the conductivity rises by many orders of magnitude. The percolation threshold was shown to shift to lower filler fractions with the decreasing particle size, because of higher probability of cluster formation and decreased average distance between the particles, which enhances tunneling conductivity [12]. The threshold concentration may be reduced (hence conductivity increased for the same volume fraction of the filler) for elongated particles, such as carbon nanofibers or carbon nanotubes [18], yet this may be of less importance at high filler contents, as in this work. Nevertheless, we tested as conductive filler materials carbon blacks (CB) of two different sizes, carbon nanofibers having a high aspect ratio, and their combinations.

Asymmetrically porous supports are prepared using the immersion precipitation (phase inversion) method, whereby spreading a polymer solution on a flat substrate (e.g., a polyester non-woven) to form a film is followed by precipitating the polymer and leaching the solvent out in a ice water bath [7]. The modified procedure used in this work replaced pure PSf solution with a concentrated CB

dispersion in a solution of PSf. The PSf and CB content in dispersion was optimized to achieve, on one hand, a good uniformity (no macroscopic aggregates), facile spreading and a smooth film surface and, on the other hand, a maximum conductivity, as described in the following section.

For the next EP deposition of the active top layer, two different monomers were investigated representing two generic groups, namely, phenol which forms electronically insulating films and aniline forming electronically conductive films. Polyphenylene oxide (PPO) obtained by EP of phenol is an attractive material, since it is chemically inert, resistant to oxidation or hydrolysis at both basic or acidic conditions, and is mechanically and thermally stable [19] and exhibits molecular size-selective permeabilities [20]. The electrochemical growth of the PPO film is self-limited due to the insulating properties of the film. As a result, films as thin as 5–10 nm may be formed [21]. In a sense, EP of phenol may be viewed as a close analogue of IP, whereby the substrate phase, instead of supplying one of the condensation monomers by diffusion, supplies or withdraws electrons for polymerization by tunneling through the film.

Electrochemically prepared polyaniline (PANI) is a conductive polymer used in various technological applications, e.g. solid electrolytic capacitors, metal protection coatings, etc. [22, 23]. Protonation (p-doping) of amino sites at low pH allows charge transfer through the film during the EP and, therefore, virtually non-restricted growth [24]. The results presented below suggest that the better control of film growth through the time of EP in the case of conductive polymers, such as PANI, may more than offset the absence of self-limitation and difficulties in preparing very thin films more easily achieved by using insulating polymers, such as PPO.

3.2 Conductive composite supports

The optimal composition for conductive support preparation contained 30% (wt) solid fraction in NMP, where the composition of the solid fraction was 53.3 %(wt) Vulcan P, 46% PSf, 0.67% PS-*b*-PB, yielding an asymmetrically porous film approximately 200 μm thick. Higher CB-PSf ratios (≥60% carbon) resulted in marginally higher conductivity, but very high viscosity hence poor spreadability of the casting mixture and brittle films. On the other hand, the total solid content (CB and PSf) of 30% in casting dispersion was optimal for pore formation yielding a high hydraulic permeability (85–100 L m^{-2} h^{-1} bar^{-1}) and appropriate pore size assessed by retention of Dextran (83–90%). These characteristics are typical for ultrafiltration (UF) membranes and NF supports [7].

The morphology of the support of optimal composition may be seen Fig. 2. Despite the presence of a large fraction of CB in the polymer (>50%), the asymmetric pore morphology (Fig. 2a) is identical to the one obtained with pure PSf solution following the same procedure and is typical for immersion precipitation [25]. A fairly uniform distribution of CB particles of diameter in the range 20–50 nm is observed in the support matrix including the important region near the top surface (Fig. 2b). Clear signs of aggregation are however observed in the top-view image (Fig. 2c), suggesting that the aggregates present in CB powder were not completely broken. Some hole-like features of diameter 5–20 nm may also be observed in Fig. 2c and may be identified as pores: this apparently agrees with the results on retention of dextran having hydrodynamic radius of about 5 nm [26]. The specific conductivity of the supports was 0.2–0.5 S cm^{-1}, which, in combination with a small pore size, provided appropriate conditions for deposition of a top layer by EP.

In the as-received CB powder individual spherical carbon particles are loosely packed into large fractal-like aggregates [15, 27] and prone to further agglomeration in dispersion. Dispersion of the native aggregates and agglomerates may be facilitated using dispersing aids. Poly(vinyl pyrrolidone) (PVP) is traditionally used as a dispersing agent for dispersing CB in polar organic solvents [28]. Block copolymers containing one block (here PS) which is soluble in the solvent (NMP) and another one

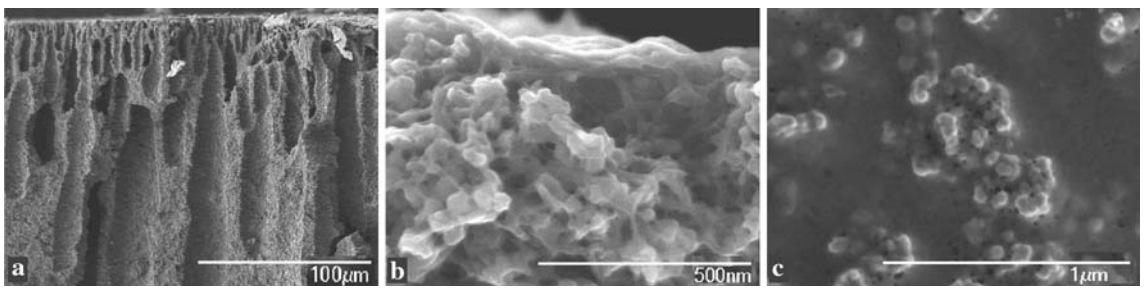

Fig. 2 HR-SEM images of freeze-fractured Vulcan P-PSf composite UF support: (**a**) cross-section showing asymmetric porous structure, (**b**) top surface region (cross-section) showing carbon particles ~20–50 nm large embedded in porous PSf matrix; (**c**) top surface showing CB aggregation and hole-like features several nm large (pores)

that is insoluble and adsorbs on the carbon surface, were also shown recently to aid and stabilize dispersion of carbon nanotubes in various solvents [29, 30]. Indeed, we found that addition of PS-*b*-PB noticeably improved uniformity and spreadability of the CB dispersion in PSf-NMP solution. Unfortunately, the conductivity of the film decreased with PS-*b*-PB content (see Fig. 3a). The same effect was observed with other types of dispersing agent (Fig. 3b). This agrees with recent reports for other CB-polymer composites [31, 32]. It was presumed that conductivity could benefit from the native CB aggregated structure and/or limited agglomeration in dispersion. However, this benefit can be lost, as the dispersants promote more complete dispersion [32]. For the same reason a similar decrease in conductivity was observed for much longer or more vigorous stirring of the dispersion [33].

A finer type of CB, Black Pearl 2000 has a higher bulk conductivity and smaller particle size compared to Vulcan P; it was expected to produce similar conductivity at lower carbon fractions [34]. However, it was found that this CB was prone to a strong agglomeration yielding highly inhomogeneous dispersions in PSf solutions and rough, brittle and visibly non-uniform films of poor conductivity (0.007–0.022 S cm^{-1} for 33–48% carbon in total solids). Despite the elongated structure, carbon nanofibers showed even poorer results. The conductivity of a film containing 47% nanofibers was only 0.002 S cm^{-1}. We presume that a likely reason was poor dispersion of nanofibers seen in SEM micrographs (not shown here). Blending with Vulcan P improved the conductivity, yet in all cases the results for both fillers were inferior to pure Vulcan P composites. It appears therefore that among the tested systems, the Vulcan P dispersion prepared using stirring (shear) and dispersants just sufficient to disperse CB aggregates but not excessively break them provided the most favorable combination of characteristics. Optimized porous CB-PSf composites were then suitable for deposition of the top layer using EP.

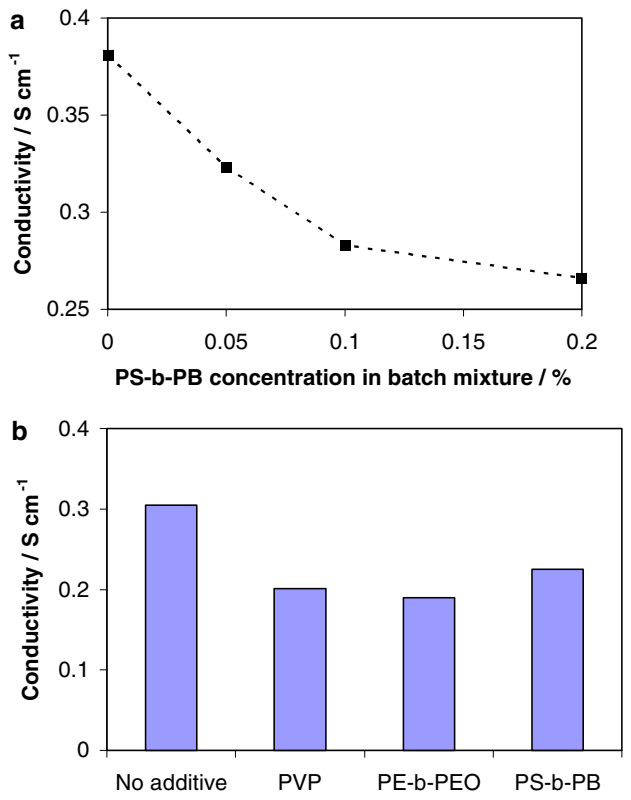

Fig. 3 Effect of addition of dispersing aids on the conductivity of porous PSf-CB films (ca. 200 μm) cast from NMP solution containing total 30% solids: (**a**) addition of PS-*b*-PB, 60% CB in solid fraction; (**b**) addition of different dispersing aids (0.2% in batch mixture), 53% CB in solid fraction

3.3 Top layer formation by EP

The EP of phenol was carried out in a 0.05 M phenol solution in 0.5 M phosphate buffer (pH 7). Prior to phenol deposition on a porous film, the occurrence of the EP reaction was verified on a solid glassy carbon disc electrode and on a dense non-porous composite film cast from the same Vulcan P-PSf dispersion. The cyclic voltammetry (CV) in Fig. 4a shows that the oxidation current rapidly decreased after the first cycle indicating passivation of the conductive surface by the growing PPO film [35]. However, a similar CV experiment with conductive porous films (Fig. 4b) showed a different pattern, with much larger currents and little or no sign of oxidation followed by passivation. This apparently results from undesired charging of the double layer adjacent to the large surface within the porous film (in the entire potential range) and oxidation of water available within the pores (at large positive potentials). However, the amount of phenol initially present within the pores is rapidly exhausted once reaction begins and may be subsequently oxidized mostly at the surface, resulting in an oxidation current commensurable with that observed for the non-porous film in Fig. 4a. In CV or potentiostatic modes, the large currents and the finite conductivity of the porous support brings about a significant potential drop along the film. Thus a significant part of the support surface might be below the minimal potential necessary for EP reaction (ca. 0.65 V, see Fig. 5a).

To achieve conditions needed for EP of phenol a galvanostatic mode was used, which allowed a slow yet steady deposition of PPO film on the top surface of the support. At 30 mA (current density 2.28 mA cm^{-2}), the potential increased first slowly then steeply due to passivation of the top surface reaching the voltage limit of the potentiostat (12 V) after about 40 min, at which point EP was stopped (Fig. 5a). The slow increase in the initial part of the chronopotentiometric chart in Fig. 5a suggests that insufficient

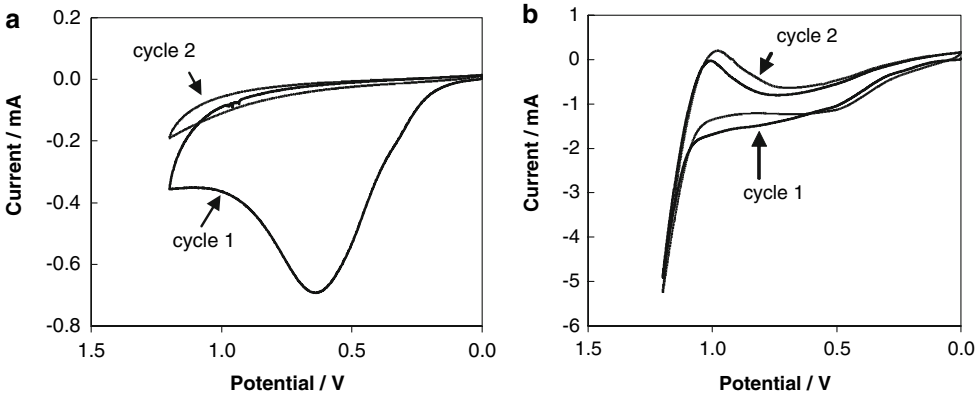

Fig. 4 Cyclic voltammetry on Vulcan P-PSf composites in 0.05 M Phenol in 0.5 M phosphate buffer: (**a**) a dense film, the phenol oxidation peak at 0.65 V disappears in the second cycle due to surface passivation by a PPO film; (**b**) porous UF composite support, large charging-discharging currents are observed

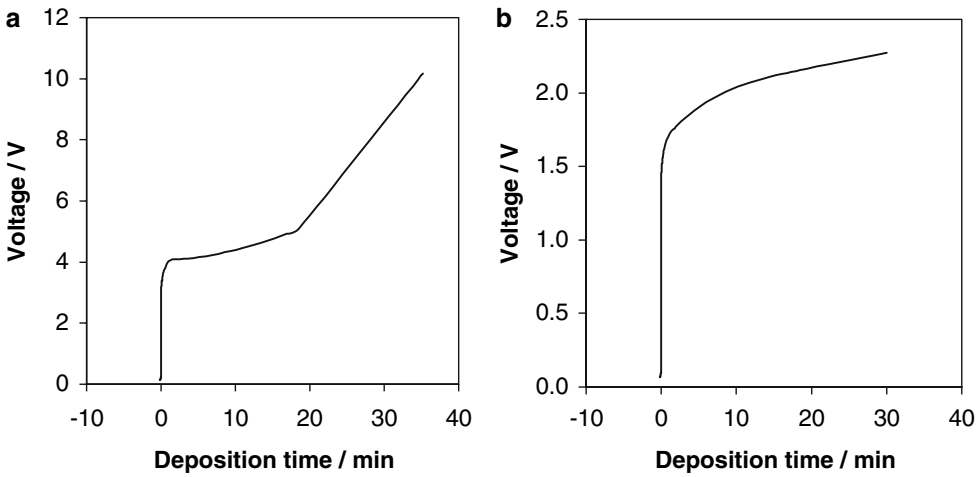

Fig. 5 Voltage diagrams of EP performed with Vulcan P-PSf composite UF support in galvanostatic regime: (**a**) 0.05 M phenol in 0.5 M phosphate buffer; (**b**) 0.05 M aniline in 0.5 M H_2SO_4 solution

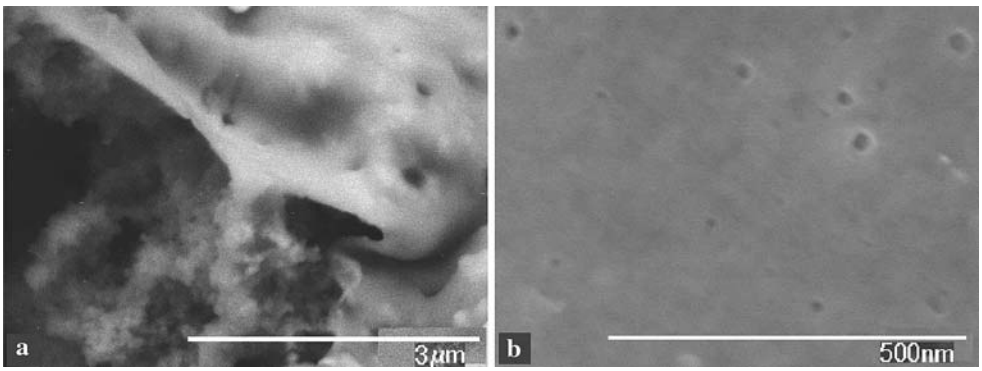

Fig. 6 HR-SEM images of a PPO film electrochemically deposited on the top of the conductive Vulcan P-PSf composite UF support. (**a**) Cross-section of the PPO film and the underlying support (seen at the bottom left). (**b**) Top surface of the PPO film; hole-like defects ~ 5–20 nm in diameter are observed

conductivity precluded uniform reaction over the whole surface, so that passivation apparently proceeded from the edges towards the middle part of the sample. Yet eventually the whole substrate surface (or at least all conductive patches at the surface) were complete sealed by the PPO film.

The cross-section and top surface of the composite membrane after PPO deposition near the center of the sample is shown in Fig. 6. The morphological change compared to the untreated porous support is clearly seen with a continuous and strongly adherent PPO layer on top of the support. Unfortunately, compared to the bare support, the membrane showed only a marginal decrease in water permeability (~24%) and zero rejection to $MgSO_4$ and sucrose, which suggests that the surface was not completely sealed. Small defects could still be seen on the surface (Fig. 6b) similar to the hole-like features observed

on the support surface (Fig. 2c). Sucrose molecules (hydraulic radius ~0.5 nm) and salt could freely pass through these defects. Apparently, the insulating PPO film could not grow over some areas on the top surface, and holes in particular, where the tunneling current was too small. Although it is apparent that PPO can be electrochemically deposited on the top of the conductive support, it will need conductive support of better uniformity and more finely and uniformly distributed conductive patches for preparation of membranes with nanofiltration characteristics.

In contrast to phenol, the growth of a polyaniline film in acidic conditions is unrestricted. In fact the deposited film improves uniformity of the whole surface and ensures absence of hole-like defects (Fig. 7) The advantage of self-limitation (as for IP and EP of phenol) does not exist, but is offset by another advantage of controlling film permeability through deposition time. As a result, a considerable retention of small solutes could be achieved in this case.

The EP of aniline was carried out with 0.05 M monomer solution in 0.5 M sulfuric acid while setting the current at 50 mA (3.78 mA cm^{-2}), which was within the reported current density window that yields the best deposition conditions and highest quality of PANI films [36]. In contrast to PPO, the chronopotentiogram (Fig. 5b) does not show a sharp increase of potential in the course of polymerization, suggesting a fairly constant rate of deposition. Not surprisingly, a sharp, more than 20-fold, reduction in water flux and substantial retention of small solutes in filtration tests was observed after PANI deposition, indicating complete sealing of the substrate surface (see Fig. 8).

A clear correlation was found between the time of EP at these conditions and the retention of both sucrose and $MgSO_4$ as shown in Fig. 8. It may be assumed that the thickness of the PANI film increases with time, yet selectivity (retention) is to a large extent a material property, therefore the improving selectivity suggests that polyamiline also underwent some chemical changes. Also, after initial sealing of the support the flux did not decrease monotonically with deposition time and, at some point, started to increase. It is not unreasonable then to assume that, concurrently with the thickness increase, the PANI film could further oxidize, which could tighten (cross-link) the polymer structure and increase selectivity, but, on the other hand, make it more polar and more permeable to water.

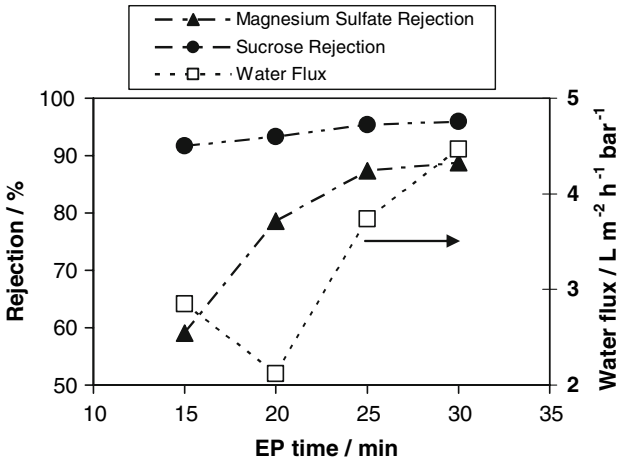

Fig. 8 Rejection of $MgSO_4$ and sucrose and water flux of membranes prepared by electrochemical deposition of PANI film on conductive Vulcan P-PSf composite UF support as a function of EP time

4 Conclusions

It was shown that a composite membrane with NF characteristics [37] could be obtained using EP on a porous conductive composite support comprised of polysulfone and carbon black particles. It is to be emphasized that the present study was mostly intended to explore the principle of using EP and breaking the monopoly of IP for making TFC NF membranes. Although the thickness of the prepared active PANI layer (100–200 nm, see Fig. 7a) was somewhat thicker than in the best commercial polyamide NF membranes (<50 nm) [38], the flux was not very far from the best available performance (5–15 L m^{-2} h^{-1} bar^{-1}) and is clearly subject to optimization. The studied materials, particularly PANI, are apparently not optimal in terms of chemical stability and selectivity, yet this may be improved by using various derivatives of these and other monomers,

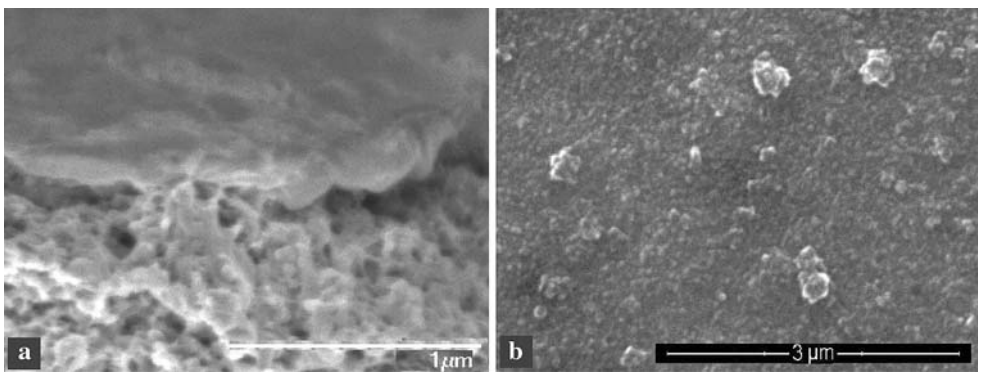

Fig. 7 HR-SEM images of a PANI film electrochemically deposited on top of the conductive Vulcan P-PSf composite support, EP time 30 min: (**a**) fractured cross-section showing PANI top layer about 100–200 nm thick; (**b**) top surface of the PANI film showing complete coverage of the support surface

as well as improved buffers and EP deposition conditions. Perhaps the most critical limiting factor is the conductivity of the support, since it determines the maximum area of the NF membrane that can be prepared in a single step. If polymer-carbon composites are to be used in the future, a change in the setup would be beneficial, e.g., current collection through rather than along the substrate, which will drastically reduce the required conductivity and carbon content, or the use of more conductive composites, e.g., involving carbon nanotubes.

Acknowledgments This work was supported by a grant from the NATAF program of the Ministry of Trade and Industry of Israel. The authors thank the electron microscopy unit of the Ilse Katz Center for Nanosciences at Ben-Gurion University and Ms. Lubov Burlaka for taking SEM images.

Appendix. Derivation of Eq. 1 for circular and rectangular geometries

Given the electrochemical cell design, i.e., a circular film of diameter D clamped at the entire edge and collecting a uniform current density i, the change in potential in the radial direction can be described by a system of differential Eqs. A1 and A2:

$$I(r) = -2\pi rh\sigma \frac{d\varphi}{dr}. \tag{A1}$$

$$dI = -2\pi rid r \tag{A2}$$

where φ is the potential, $I(r)$ the current flowing through the film in the radial direction at radial position r, h the film thickness, and σ is the specific conductivity of the film. From the radial symmetry $I(0) = 0$, then at $r = D/2$, we solve Eqs. A1 and A2 to obtain

$$\Delta\varphi = \varphi(r = D/2) - \varphi(r = 0) = \frac{iD^2}{16\sigma h} \tag{A3}$$

where $\Delta\varphi$ is the potential drop from the current collector to the center of the circular anode and D is the diameter of the anode. For a rectangular film of length L clamped (connected to the same current collector) at the opposite edges, r and $2\pi r$ in Eqs. A1 and A2 are replaced with x (length coordinate) and a constant width W, respectively, and, after integrating from $x = 0$ (the center of the film) to $x = L/2$ (the edge), Eq. A3 is replaced with

$$\Delta\varphi = \frac{iL^2}{8\sigma h}, \tag{A4}$$

References

1. Rautenbach R, Gröschl A (1990) Desalination 77:73
2. Van der Bruggen B, Schaep J, Wilms D, Vandecasteele C (1999) J Memb Sci 156:29
3. Schaefer A, Fane A, Waite T (2002) Nanofiltration principles and applications. Elsevier, Oxford, UK
4. Petersen RJ (1993) J Memb Sci 83:81
5. Vankelekom IFJ, De Smet K, Gevers L, Jacobs PA (2004) In: Schaefer A, Fane A, Waite T (eds) Nanofiltration principles and applications. Elsevier, Oxford, UK
6. Amjad Z (1993) Reverse osmosis: Membrane technology, water chemistry and industrial applications. Chapman & Hall, New York, USA
7. Mulder M (1996) Basic principles of membrane technology. Kluwer Academic Publishers, Dordrecht
8. Bellona C, Drewes J, Xua P, Amy G (2004) Water Res 38:2795
9. Agenson K, Oh J, Urase T (2003) J Memb Sci 225:91
10. Lund H, Hammerich O (2001) Organic electrochemistry. Marcel Dekker, New York, USA
11. Mantell CL (1968) Carbon and graphite handbook. Interscience Publishers
12. Ezquerra TA, Connor MT, Roy S, Kulescza M, Fernandes-Nscimento J, Balta-Calleja FJ (2001) Compos Sci Technol 61:903
13. Barkauskas J, Vinslovaite A (2003) Mater Res Bull 38:1437
14. Heaney MB (1997) Physica A 241:296
15. Jaeger KM, McQueen DH (2001) Polymer 42:9575
16. Zhao Z, Yu W, He X, Chen X (2003) Mater Lett 57:3082
17. Ishigure Y, Iijima S, Ito H, Ota T, Unuma H, Takahashi M, Hikichi Y, Suzuki H (1999) J Mater Sci 34:2979
18. Regev O, ElKati PNB, Loos J; Koning C E (2004) Adv Mater 16:248
19. Mengoli G, Musiani M (1987) J Electrochem Soc 134:643C
20. McCarley R, Irene E, Murray R (1991) J Phys Chem 95:2492
21. Roser S, Caruana D, Gerstenberg M (1996) J Electroanal Chem 411:153
22. Kanungo M, Kumar A, Contractor A (2002) J Electroanal Chem 528:46
23. Sazou D, Georgolios C (1997) J Electroanal Chem 429:81
24. Yano J, Ohnishi T, Kitani A (1999) Synth Met 101:752
25. Stropnik C, Kaiser V (2002) Desalination 145:1
26. Armstrong JK, Wenby RB, Meiselman HJ, Fisher TC (2004) Biophys J 87:4259
27. Eltekova NA, Razd'yakonova GI, Eltekov YuA (1993) Pure Appl Chem 65:2217
28. Cabot Corporation (1989) Carbon black dispersion, technical report S-131. Special Blacks Division of Billerica, MA, USA
29. Bandyopadhyaya R, Nativ-Roth E, Regev O, Yerushalmi-Rozen R (2002) Nano Lett 2:25
30. Shvartzman-Cohen R, Levi-Kalisman Y, Nativ-Roth E, Yerushalmi-Rozen R (2004) Langmuir 20:6085
31. Grossiord N, Loos J, Regev O, Koning CE (2006) Chem Mater 18:1089
32. Grunlan JC, Bloom FL, Gerberich WW, Francis LF (2001) J Mater Sci Lett 20:1523
33. Bigg DM (1984) J Rheology 28:501
34. Luo S, Wong C (2000) IEEE Trans Compon Pack Technol 23:151
35. Skowronski JM, Krawzyk P (2004) J Solid State Electrochem 8:442
36. Camalet J-L, Lacroix J-C, Dung Nguen T, Aeiyach S, Pham MC, Petitjean J, Lacaze P-C (2002) J Electroanal Chem 485:13
37. Koros W J, Ma YH, Shimidzu T (1996) J Memb Sci 120:149
38. Freger V (2003) Langmuir 19:4791